



SEGMENTATION AND RECONSTRUCTION OF ABDOMINAL AORTIC ANEURYSM SURFACE MODELS TOWARDS THE CREATION OF IN SILICO PATIENT COHORTS

Christos MANOPOULOS, Anastasios RAPTIS, Christos PLAVOUKOS, Evangelia KRINI, Vasiliki PERIVOLIOTI, Vaia Despoina KARAGEORGOU, Konstantinos MOULAKAKIS, Ioannis KAKISIS, Nikolaos VAXEVANIDIS

***Abstract:** The aim of this study was to create a repository consisting of 3D surface models of abdominal aortic aneurysms (AAA) before and after endovascular aneurysm repair (EVAR). Computed tomography scans of 14 patients were utilized for this purpose. The workflow involved segmenting and reconstructing the medical images using Mimics software, along with several post-processing steps for surface refinement. The AAA cases encompassed the suprarenal abdominal aorta, including the celiac axis, superior mesenteric artery, and renal arteries, as well as the infrarenal abdominal aorta, including the aortic bifurcation and the common iliac arteries. The collection of patient-specific 3D AAA models will aid in the creation of virtual patient cohorts using statistical shape modeling and machine/deep learning algorithms. These models will help identify correlations between nonstandard morphometrics and clinical events, such as AAA rupture and post-EVAR complications.*

***Key words:** abdominal aortic aneurysm, endovascular aneurysm repair, computed tomography angiography, vessel reconstruction, vessel geometry modeling, vessel surface processing*

1. INTRODUCTION

Abdominal aortic aneurysm (AAA) is a medical condition characterized by the dilatation and outward swelling of the wall of the abdominal aorta. Older people and those with certain risk factors are the most vulnerable to AAA disease [1].

In men, the disease typically manifests around the age of 50 and reaches its highest frequency around the age of 80. In women, the disease appears later, but similarly exhibits a progressively increasing frequency as age advances. The estimated prevalence of AAA is derived from studies conducted in the general population, as well as screening programs for asymptomatic AAA, which report an occurrence rate ranging from 1.9% to 18.5% in men and 0% to 4.2% in women. [2] Two independent studies conducted by Singh et al. [3] in Norway and Boll et al. [4] in the Netherlands have shown that AAA with a diameter larger than 4 cm is observed in only 1% of men aged 55-64 years, with a notable increase in the percentage by 2-

4% for each successive decade. The current prevalence of AAA in men over the age of 65 has been reported to be between 1.3% and 5%. [5] If left untreated, the AAA disease can become hazardous, while timely diagnosis and appropriate medical care can prove lifesaving. Some aneurysms may require surgical intervention, most commonly via endovascular repair (EVAR) in which a stent graft is installed into the aneurysm [6].

The creation of vessel surface models, particularly for the abdominal aorta or AAAs, has been a topic of increasing interest in recent years due to its applications in various fields of biomedical engineering [7]. These anatomically accurate 3D models serve as vital resources for computational fluid dynamics (CFD), finite element analyses (FEA), or complex fluid-solid interaction (FSI) simulations [8], allowing researchers to investigate the morphological [9], hemodynamic, and biomechanical factors that contribute to the onset, growth [10], and rupture of AAAs on a patient-specific basis [11].

Furthermore, these 3D anatomical models greatly aid biomedical engineers in the development of medical devices and implants, often tailored and customized to meet the specific medical requirements of individual patients. Critical insights can be gained for surgical planning, particularly for complex cases involving juxtarenal, suprarenal, or thoracoabdominal aortic aneurysms [12]. These complex geometries often require custom stent-graft systems, as standard commercial devices may not conform to such intricate structures. The use of 3D printing technology to create physical models based on the reconstructed 3D virtual models is also gaining prominence in clinical research [13] and the training of vascular surgeons [14].

Segmentation is the first step in creating 3D vascular models from medical images. This process involves isolating the blood vessels of interest from the rest of the image using various techniques such as thresholding, edge detection, and region growing [15]. Accurate segmentation is critical as it sets the foundation for the subsequent steps. Once the vessels are segmented, the next step is reconstruction, where the 2D image data is converted into 3D models using various algorithms such as marching cubes, voxelization, or curve-based modeling. The goal of reconstruction is to create a smooth, continuous 3D surface mesh that represents the blood vessels. Post-processing is the final step, where the resulting 3D model is refined and optimized for visualization, analysis, or simulation. This may involve removing noise, smoothing the surface, or adding texture to enhance realism.

There are several specialized software packages, either commercial or not, available for creating 3D models from medical imaging data, such as ImageJ, ITK-SNAP [16], 3D Slicer [17], Visualization Toolkit (VTK) [18], Vascular Modelling Toolkit (VMTK), and Mimics (Materialise Inc. Leuven, Belgium). The latter software, used in the present study, offers a wide range of tools that facilitate the precise modeling of anatomic structures, enhancing the accuracy and detail of the resulting 3D models.

The current pilot study is specifically dedicated to the 3D surface modelling of AAAs in real patients, both pre- and post- EVAR.

While most computational studies that involve 3D vascular models (or AAA models more specifically) mostly do not disclose the specific methods/tools used, this study aim to furnish practical guidance on the segmentation, reconstruction, and post-processing of patient-specific AAA models.

2. MATERIALS AND METHODS

The patient cohort that was considered in the current study consists of 14 cases possessing medical imaging data before (applicable to all cases) and after EVAR (applicable to 4 out of the 14 cases). The anonymized CT scans were provided by the Vascular Surgery Clinic of the "Attikon" General University Hospital, which is affiliated to the School of Medicine, National and Kapodistrian University of Athens, Greece. Prior to the secondary use of the medical imaging data for research purposes, the study received ethical approval from the Ethics Committee. More information about the patients with respect to basic demographics and stent-grafts installed (where applicable), is provided in Table 1, while several geometrical characteristics of all the AAAs before EVAR are tabulated in Table 2.

Table 1.

Patient cohort data.

| No. | Gender | Age (y.o.) | EVAR Grafts |
|-----|--------|------------|-------------------------------|
| 1 | Male | 81 | Lower profile EXCLUDER (GORE) |
| 2 | Male | 89 | - |
| 3 | Male | 72 | - |
| 4 | Male | 66 | - |
| 5 | Female | 67 | - |
| 6 | Male | 63 | - |
| 7 | Male | 57 | EXCLUDER (GORE) |
| 8 | Male | 57 | - |
| 9 | Male | 70 | - |
| 10 | Male | 75 | Zenith (COOK) |
| 11 | Male | 81 | - |
| 12 | Male | 76 | - |
| 13 | Male | 65 | Zenith (COOK) |
| 14 | Female | 69 | - |

Table 2.
Basic geometrical measurements (all in mm) of AAAs preoperatively.

| No | Neck diam. | AAA diam. | AAA length | Left iliac diam. | Right iliac diam. |
|----|------------|-----------|------------|------------------|-------------------|
| 1 | 21 | 48 | 69 | 11 | 10 |
| 2 | 24 | 75 | 78 | 12 | 14 |
| 3 | 22 | 51 | 74 | 9 | 11 |
| 4 | 30 | 58 | 68 | 22 | 20 |
| 5 | 19 | 44 | 49 | 8 | 10 |
| 6 | 25 | 48 | 80 | 13 | 13 |
| 7 | 21 | 68 | 83 | 16 | 20 |
| 8 | 21 | 48 | 101 | 20 | 15 |
| 9 | 24 | 50 | 64 | 10 | 10 |
| 10 | 19 | 52 | 55 | 11 | 11 |
| 11 | 20 | 50 | 67 | 15 | 12 |
| 12 | 26 | 55 | 81 | 13 | 15 |
| 13 | 24 | 52 | 135 | 13 | 12 |
| 14 | 21 | 62 | 44 | 11 | 12 |

2.1 Modelling

For each case, the first step in the segmentation and reconstruction procedure was the inspection of the CT scans and the selection of the most suitable imaging series to be further processed, in terms of quality, number of slices, slice thickness and spacing, pixel size and resolution. The use of contrast agent is typical in the pre- and post-operative medical imaging examination (via CT) of AAA patients as it improves visibility and facilitates accurate assessment of sharp changes in lumen diameter (especially around the aneurysmal bulge) as well as the extend of intraluminal thrombus and calcified areas on the aortic wall. Any contrast-enhanced CT scans were favored over non-contrast-enhanced CT scans, where applicable.

The target of the reconstruction involved not only the aneurysmal bulge but also the upstream vasculature including the celiac axis, the superior mesenteric and the renal arteries, as well as part of the downstream vasculature, i.e. the common iliac arteries up to their bifurcation.

The selected image series for each case consists of 2D medical images in DICOM format, which were imported in Mimics software. After creating a “new project” within Mimics, the brightness and contrast threshold values were adjusted to better visualize internal tissues and organs. It is pointed out that in many cases it was necessary to adjust the colors of the

CT images using the "Pseudo Colors" option, to better visualize the aortic lumen.

Mimics software provides convenient and efficient tools to perform an initial rough segmentation of the region of interest (the abdominal aorta and branching arteries in our case). Using the "dynamic region grow" tool, a primary raw mask was generated and underwent necessary processing and smoothing to better fit the target structure (the lumen) as presented on each slice (on each 2D DICOM image), employing the tools: “Smart Fill”, "Smooth Mask" (smoothing the outer surface), "Fill Cavities" (covering internal holes), and "Edit Masks" (locally adding/drawing or removing/erasing parts of the existing mask, and adjusting the diameter for the tool “working surface” to be more accurate during the adjustment of the “active” surface of the mask).

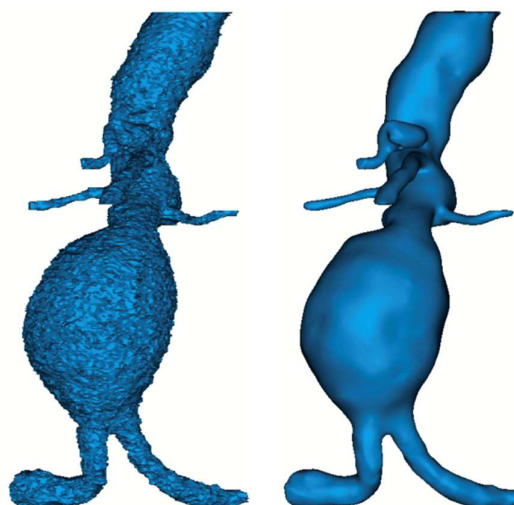


Fig.1. Indicative 3D model before and after surface processing and smoothing

The resulting improved mask served as the final raw representation and was further employed to create a preliminary 3D model, which would be further processed as described below.

Due to the low resolution of some image series, the final 2D mask was not as accurate as expected in some cases. It was necessary in these cases to use an additional automated mask expansion tool called "Flood Fill", which conducts local mask expansion through the luminance threshold, and simultaneous merging with the adjacent arteries that had been formed

under the main mask. Subsequently, the preliminary 3D model, after being visually inspected and evaluated, was processed again using initially the 'Wrap' and then the 'Smooth' command. The 'Wrap' command slightly inflates

was eventually obtained with the aforementioned surface processing strategy.

Also, it is noted that each case needed a different “working” approach in constructing the 3D model, in terms of the sequence of processes

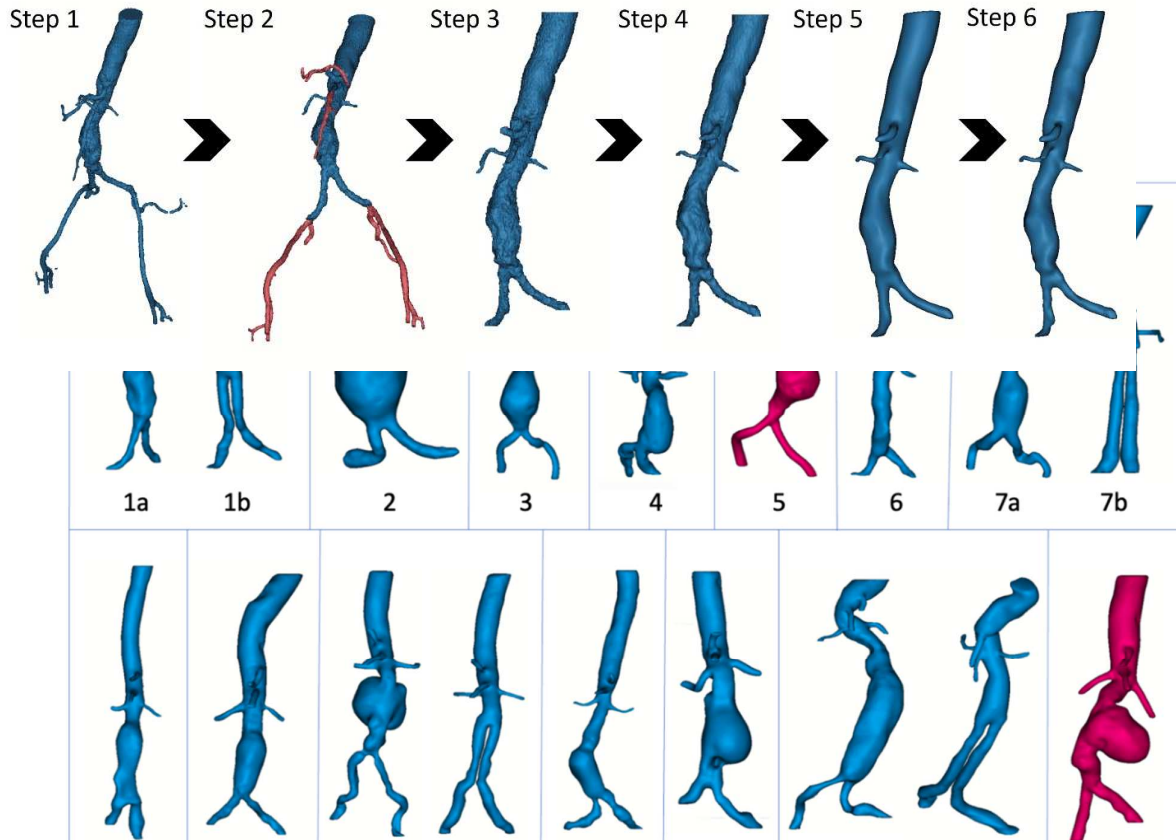


Fig.2. Final 3D patient’s models after processing. Male patients are represented in blue, while female patients are represented in red. Cases presented with the letters “a” and “b” correspond to the pre- and post-EVAR structures accordingly

the 3D model and the 'Smooth' command smooths the outer (inflated) surface. The result of this iterative “swelling-smoothing” process, after multiple tests performed in the Mimics environment, was the formation of a smoother 3D representation of the aortic lumen (a lot smoother than the representation that would have been created if the mask had been overly expanded in the 2D plane first and then overly smoothed, via imposing large smoothing coefficients, in the 3D setting. Thus, both a more accurate 3D approach (with respect to the real abdominal aorta model), and at the same time a smoother 3D mesh with fewer imperfections

that was followed. More specifically, it was sometimes necessary, both to change the (scalar valued) parameters defined in the various tools, and to execute some commands several times until a smooth yet morphology-preserving external surface could be obtained.

Additionally, it is particularly important to mention that in some cases that had very few CT images available, it was necessary to manually create sub 3D sections and models of the main aortic lumen and the considered aortic branches (through individual masks and by using the “Split mask” command) and join them into a single final model, after processing each part separately.

Fig.3. Surface processing steps followed in case 1a as described in the corresponding table in paragraph 2.2

Finally, at the end of the modeling process, the "Edit Contours" command was used on all final 3D models, for the detailed improvement of the external surface of each model manually. With this tool, it was possible to locally "manipulate" the surface of the outer contour of the model (in all views: coronal, axial, and sagittal) and also to perform local smoothing where needed.

2.2 Procedures performed in each case

| | |
|---------|---|
| 1a | 1. Raw mask creation and processing of initial surface. 2. Edit mask and split mask in various parts. 3. Processing of main aorta lumen with "edit mask", "Flood fill" (in some mask parts) and Multiple slice edit. 4. Creation of first 3D model. 5. Processing of model with wrapping and smoothing (3 times). 6. 3D model processed via edit contours. 7. Exported final 3D model as an STL file. |
| 1b | Same as patient 1a until the export of the first 3D model. Then, a 3D section was created between the attached iliac arteries, removed from the original 3D model using minus Boolean operation command to separate them in the final model. Final model processed and exported as an STL file. |
| 2 | Same as patient 1a, but wrapping and smoothing procedures performed twice. |
| 3 & 4 | Same main procedures as patient 1a, but each part processed separately due to uneven narrowing of smaller arteries. Final consolidated model created using the "merge" procedure. |
| 5 & 6 | Same as patient 1a, but wrapping and smoothing procedures performed twice. |
| 7a & 7b | Same as patient 3 and 4. |

| | |
|-------|--|
| 8 & 9 | Same as patient 1a, but wrapping and smoothing procedures performed twice. |
| 10a | Same as patient 1a. |
| 10b | Same as patient 3 and 4. |
| 11 | Same as patient 1a, but wrapping and smoothing procedures performed twice. |
| 12 | Same as patient 1a. |
| 13a | Same as patient 1a, but wrapping and smoothing procedures performed twice. |
| 13b | Same as patient 3 and 4. |
| 14 | Same as patient 1a, but wrapping and smoothing procedures performed twice. |

3. RESULTS & DISCUSSION

The whole set of 3D models, obtained after processing the CT scan data, are presented in Figure 2. The post-EVAR 3D model was created only for patients 1, 7, 10 and 13 who had the relevant imaging data available.

A repository of 3D patient-specific AAA models serves multiple purposes in studying this disease. One specific application is statistical shape modeling (SSM), a mathematical technique that analyzes the variation in the shape of the AAA anatomy within a population. To accomplish this, a principal component analysis (PCA) is conducted, which provides independent components that describe the shape variation. These components capture potential relationships between different morphological characteristics. SSM can reveal geometrical characteristics that may not be readily apparent through manual calculations of traditional morphological features. Indicatively, van Veldhuizen et al. [19] have developed a SSM focusing on the infrarenal AAA neck contributing to the definition of a hostile neck anatomy which has not been formally defined in the literature [20]. The anatomy of the AAA neck plays a crucial role in the success of an EVAR procedure as it serves as the landing zone for stent-grafts. Geometrical factors such as the neck length, diameter and angulation, determine

whether the stent-graft can be securely fixated and sealed.

As a future quest, we are planning to develop SSM for the whole AAA structure and attempt to correlate intricate geometrical characteristics with AAA growth and rupture events, as well as post-EVAR complications [21]. Moreover, SSM will allow the creation of extended virtual patient cohorts enclosing several and diverse (in terms of morphology) AAA cases. The lack of accessible real patient data hampers most research attempts, especially with respect to AAA disease. Such virtual patient cohorts, created by SSM employing smaller real patient cohorts, seems an efficient solution to advance research on this life-threatening disease, which has been characterized as a “silent killer”.

4. CONCLUSIONS

In summary, this study provides a comprehensive framework for the segmentation, reconstruction, and post-reconstruction surface processes essential for creating 18 patient-specific AAA models, both pre- and post-intervention. Unlike existing computational research focused primarily on AAA hemodynamics or arterial wall mechanics, our work fills a critical knowledge gap by elucidating the practical steps involved in the initial development of these 3D models. In future iterations of this research, we plan to integrate SSM and leverage advanced machine learning or deep learning algorithms to construct virtual patient cohorts. This methodological enhancement aims to accelerate and deepen the understanding about AAAs.

5. REFERENCES

- [1] Sakalihasan, N., Limet, R., Defawe, O., *Abdominal aortic aneurysm*, *The Lancet*, vol. 365, no. 9470, pp. 1577–1589, 2005, [https://doi.org/10.1016/s0140-6736\(05\)66459-8](https://doi.org/10.1016/s0140-6736(05)66459-8).
- [2] Ullery, B.W., Hallett, R.L., Fleischmann, D., *Epidemiology and contemporary management of abdominal aortic aneurysms*, *Abdom. Radiol.*, vol. 43, pp. 1032–1043, 2018.
- [3] Singh, K., Bønaa, K.H., Jacobsen, B.K., Bjørk, L., Solberg, S., *Prevalence of and risk factors for abdominal aortic aneurysms in a population-based study: The Tromsø Study*, *Am. J. Epidemiol.*, vol. 154, no. 3, pp. 236–244, 2001.
- [4] Boll, A.P.M., Verbeek, A.L.M., Van de Lisdonk, E.H., Van der Vliet, J.A., *High prevalence of abdominal aortic aneurysm in a primary care screening programme*, *J. Br. Surg.*, vol. 85, no. 8, pp. 1090–1094, 1998.
- [5] Naylor, A.R., et al. *European society for vascular surgery (ESVS) 2023 Clinical practice guidelines on the management of atherosclerotic carotid and vertebral artery disease*, *Eur. J. Vasc. Endovasc. Surg.*, 2022, <https://doi.org/10.1016/j.ejvs.2022.04.011>
- [6] White, V., Wyatt, M., *Endovascular treatment of abdominal aortic aneurysms*, *Surg. Oxf.*, vol. 33, no. 7, pp. 334–339, 2015, <https://doi.org/10.1016/j.mpsur.2015.04.004>.
- [7] Wu, J., Hu, Q., Ma, X., *Comparative study of surface modeling methods for vascular structures*, *Comput. Med. Imaging Graph.*, vol. 37, no. 1, pp. 4–14, Jan. 2013, <https://doi.org/10.1016/j.compmedimag.2013.01.002>.
- [8] Xenos, M., Rambhia, S.H., Alemu, Y., Einav, S., Labropoulos, N., Tassiopoulos, A., Ricotta, J.J., Bluestein, D., *Patient-Based Abdominal Aortic Aneurysm Rupture Risk Prediction with Fluid Structure Interaction Modeling*, *Ann. Biomed. Eng.*, vol. 38, no. 11, pp. 3323–3337, 2010, <https://doi.org/10.1007/s10439-010-0094-3>.
- [9] Shum, J., Martufi, G., Martino, E.D., Washington, C.B., Grisafi, J., Muluk, S.C., Finol, E.A., *Quantitative Assessment of Abdominal Aortic Aneurysm Geometry*, *Ann. Biomed. Eng.*, vol. 39, no. 1, pp. 277–286, 2011, <https://doi.org/10.1007/s10439-010-0175-3>.
- [10] Humphrey, J.D., Holzapfel, G.A., *Mechanics, mechanobiology, and modeling of human abdominal aorta and aneurysms*, *J. Biomech.*, vol. 45, no. 5, pp. 805–814, 2012, <https://doi.org/10.1016/j.jbiomech.2011.11.021>.
- [11] Gasser, T.C., Miller, C., Polzer, S., Roy, J., *A quarter of a century biomechanical rupture risk assessment of abdominal aortic*

- aneurysms. Achievements, clinical relevance, and ongoing developments*, Int. J. Numer. Methods Biomed. Eng., p. e3587, 2022, <https://doi.org/10.1002/cnm.3587>.
- [12] Moulakakis, K.G., Kakisis, J., Gonidaki, E., Lazaris, A.M., Tsangaris, S., Geroulakos, G., Manopoulos, C., *Comparison of Fluid Dynamics Variations Between Chimney and Fenestrated Endografts for Pararenal Aneurysms Repair: A Patient Specific Computational Study as Motivation for Clinical Decision-Making.*, Vasc. Endovascular Surg., vol. 53, no. 7, pp. 572–582, 2019, <https://doi.org/10.1177/1538574419867531>.
- [13] Willson, K., Atala, A., *Medical 3D Printing: Tools and Techniques, Today and Tomorrow*, Annu. Rev. Chem. Biomol. Eng., vol. 13, no. 1, 2022, <https://doi.org/10.1146/annurev-chembioeng-092220-015404>.
- [14] Coles-Black, J., Bolton, D., Chuen, J., *Accessing 3D Printed Vascular Phantoms for Procedural Simulation*, Front. Surg., vol. 7, p. 626212, 2021, <https://doi.org/10.3389/fsurg.2020.626212>.
- [15] Lesage, D., Angelini, E.D., Bloch, I., Funke-Lea, G., *A review of 3D vessel lumen segmentation techniques: Models, features and extraction schemes*, Med. Image Anal., vol. 13, no. 6, pp. 819–845, Dec. 2009, <https://doi.org/10.1016/j.media.2009.07.011>.
- [16] Yushkevich, P.A., Piven, J., Hazlett, H.C., Smith, R.G., Ho, S., Gee, J.C., Gerig, G., *User-guided 3D active contour segmentation of anatomical structures: Significantly improved efficiency and reliability*, NeuroImage, vol. 31, no. 3, pp. 1116–1128, Jul. 2006, <https://doi.org/10.1016/j.neuroimage.2006.01.015>.
- [17] Fedorov, A., Beichel, R., Kalpathy-Cramer, J., Finet, J., Fillion-Robin, J.-C., Pujol, S., Bauer, C., Jennings, D., Fennessy, F., Sonka, M., Buatti, J., Aylward, S., Miller, J.V., Pieper, S., Kikinis, R., *3D Slicer as an Image Computing Platform for the Quantitative Imaging Network*, Magn. Reson. Imaging, vol. 30, no. 9, pp. 1323–1341, Nov. 2012, <https://doi.org/10.1016/j.mri.2012.05.001>.
- [18] Schroeder, W., Martin, K., Lorensen, B., *The visualization toolkit (4th ed.)*. Kitware, 2006.
- [19] Veldhuizen, W.A. van, Schuurmann, R.C.L., Ijpma, F.F.A., Kropman, R.H.J., Antoniou, G.A., Wolterink, J.M., Vries, J.-P.P.M. de, *A Statistical Shape Model of the Morphological Variation of the Infrarenal Abdominal Aortic Aneurysm Neck*, J. Clin. Med., vol. 11, no. 6, p. 1687, 2022, <https://doi.org/10.3390/jcm11061687>.
- [20] Marone, E.M., Freyrie, A., Ruotolo, C., Michelagnoli, S., Antonello, M., Speziale, F., Veroux, P., Gargiulo, M., Gaggiano, A., *Expert Opinion on Hostile Neck Definition in Endovascular Treatment of Abdominal Aortic Aneurysms (a Delphi Consensus)*, Ann. Vasc. Surg., vol. 62, pp. 173–182, Jan. 2020, <https://doi.org/10.1016/j.avsg.2019.05.049>.
- [21] Mantas, G.K., Antonopoulos, C.N., Sfyroeras, G.S., Moulakakis, K.G., Kakisis, J.D., Mylonas, S.N., Liapis, C.D., *Factors Predisposing to Endograft Limb Occlusion after Endovascular Aortic Repair*, Eur. J. Vasc. Endovasc. Surg., vol. 49, no. 1, pp. 39–44, 2015, <https://doi.org/10.1016/j.ejvs.2014.09.012>

Segmentarea și reconstrucția modelelor de suprafață a aneurismului aortic

Scopul acestui studiu a fost de a crea un depozit format din modele de suprafață 3D ale aneurismelor de aortă abdominală (AAA) înainte și după vindecarea aneurismului endovascular (EVAR). În acest scop, au fost utilizate tomografiile computerizate a 18 pacienți. Fluxul de lucru a implicat segmentarea și reconstrucția imaginilor medicale folosind software-ul Mimics, împreună cu mai mulți pași de post-procesare pentru rafinarea suprafeței [1]. Cazurile de AAA au cuprins aorta abdominală suprarenală, inclusiv axa celiacă, artera mezenterică superioară și arterele renale, precum și aorta abdominală infrarenală, inclusiv bifurcația aortică și arterele iliace comune. Colecția de modele 3D AAA specifice

pacientului va ajuta la crearea de cohorte de pacienți in silico folosind modelarea statistică a formei [2,3] și algoritmi de învățare automată/deep learning [4]

Christos MANOPOULOS, M.Sc.E., PhD Assistant Professor, Laboratory of Biofluid Mechanics and Biomedical Technology, Fluids Section, School of Mechanical Engineering, National Technical University of Athens, Greece, manopoul@central.ntua.gr

Anastasios RAPTIS, PhD Laboratory Teaching Staff, Laboratory of Biofluid Mechanics and Biomedical Technology, Fluids Section, School of Mechanical Engineering, National Technical University of Athens, Greece, raptistasos@mail.ntua.gr

Christos PLAVOUKOS, Undergraduate Student, Laboratory of Manufacturing Processes and Machine Tools (LMProMaT), School of Pedagogical and Technological Education (ASPETE), Greece, 18chr.plav@mec.aspete.gr

Evangelia KRINI, Undergraduate Student, Laboratory of Manufacturing Processes and Machine Tools (LMProMaT), School of Pedagogical and Technological Education (ASPETE), Greece, 18eva.krin@mec.aspete.gr

Vasiliki PERIVOLIOTI, Undergraduate Student, Laboratory of Manufacturing Processes and Machine Tools (LMProMaT), School of Pedagogical and Technological Education (ASPETE), Greece, 18vas.peri@mec.aspete.gr

Vaia Despoina KARAGEORGOU, Undergraduate Student, Laboratory of Manufacturing Processes and Machine Tools (LMProMaT), School of Pedagogical and Technological Education (ASPETE), Greece, 18vai.kara@mec.aspete.gr

Konstantinos MOULAKAKIS, MD, PhD, MSc, FEBVS, Associate Professor, Department of Vascular Surgery, School of Medicine, University of Patras, Greece, konmoulakakis@yahoo.gr

Ioannis KAKISIS, MD, PhD, MSc, FEBVS, Professor, Department of Vascular Surgery, Attikon University Hospital, National and Kapodistrian University of Athens, Greece, kakisis@med.uoa.gr

Nikolaos VAXEVANIDIS, Professor, Laboratory of Manufacturing Processes and Machine Tools (LMProMaT), School of Pedagogical and Technological Education (ASPETE), Greece, vaxev@aspete.gr